

Anomalous diffraction theory for arbitrarily oriented finite circular cylinders and comparison with exact T -matrix results

Yangang Liu, W. Patrick Arnott, and John Hallett

A general method is developed to formulate extinction and absorption efficiency for nonspherical particles at arbitrary and random orientations by use of anomalous diffraction theory (ADT). An ADT for finite circular cylinders is evaluated as an example. Existing ADT's for infinite cylinders at arbitrary orientations and for finite cylinders at the normal incidence are shown to be special cases of the new formulation. ADT solutions for finite cylinders are shown to approach the rigorous T -matrix results when the refractive indices approach unity. The importance of some physical processes that are neglected in the ADT approximation are evaluated by comparisons between ADT and rigorous calculations for different particle geometries. For spheres, van de Hulst's ADT and Mie theory are used, whereas the ADT that we present and T -matrix calculations are used for cylinders of different diameter-to-length ratios. The results show that the differences in extinction between ADT and exact solutions generally decrease with nonsphericity. A similar decrease occurs for absorption at wavelengths of relatively strong absorption. The influence of complex refractive index is evaluated. Our results suggest that ADT may provide a useful approximation in parameterization and remote sensing of cirrus clouds in the Christiansen bands where the real part of the refractive index approaches unity and/or where relative absorption is strong. © 1998 Optical Society of America

OCIS codes: 010.1290, 010.1310, 290.2200, 290.4020, 290.5850.

1. Introduction

Knowledge of scattering by particles is required in many applications that involve electromagnetic waves passing through a particulate cloud. For example, extinction and absorption efficiency of ice crystals are required for studying cloud effects on climate.¹⁻³ These quantities are also critical for retrieving particle properties such as size distributions from optical measurements.⁴ Because aerosol particles and ice crystals are generally nonspherical, nonspherical scattering has been an area of active research, and a number of approaches have been developed. The computational efficiency of the T -matrix method has recently been improved, enhancing the utility of this method for calculating the exact scattering properties of certain axisymmetric particles.⁵ Even with this improvement, the compu-

tation is impractical for particles that are large relative to a wavelength and/or have extreme geometry.^{5,6} Simple approximations to these complicated solutions are desirable.

Many studies have approximated nonspherical scattering by applying Mie theory to the corresponding volume- or surface-equivalent spheres. However, researchers have increasingly recognized that the light-scattering properties of nonspherical particles can differ significantly from those of such equivalent spheres, and use of Mie solutions for equivalent spheres may cause serious errors in applications such as remote sensing.^{1-3, 7-10} For example, the discrepancy between *in situ* measurements of crystal size and retrieved crystal size from infrared radiometric measurements has led to a debate over the existence of small crystals and their role in radiation transfer.¹¹ Recognizing that the retrieval was based on Mie theory for equivalent spheres, it was argued that such discrepancy may be caused by the inappropriate treatment of nonspherical scattering in the approximation of equivalent spheres.^{1,11} In a recent numerical experiment, we inverted ice crystal size distributions from multispectral extinction measurements by applying Mie theory to ice spheres, and the

The authors are with the Atmospheric Sciences Center, Desert Research Institute, Reno, Nevada 89506.

Received 23 December 1997; revised manuscript received 13 March 1998.

0003-6935/98/215019-12\$15.00/0

© 1998 Optical Society of America

modeled extinction closely agreed with the measured values.¹² The results of this numerical study imply that the incorrect representation of particle shape may be transformed into an incorrect size distribution of ice crystals, without much loss of agreement between modeled and measured optical depth.

Another commonly used approximation is the anomalous diffraction theory (ADT) of van de Hulst.¹³ ADT has been widely used in studying scattering properties and radiative effects of cirrus clouds on climate.^{2,14} New research on ADT is directed toward modifying van de Hulst's original theory to extend the range of its applicability¹⁵⁻¹⁷ and toward formulating ADT for nonspherical particles.^{14,18-24} ADT is drawing increased attention as a potentially better approximation for nonspherical ice crystals than commonly used equivalent spheres.^{1,11} However, ADT is currently available only for spheres,¹³ spheroids,^{18,19} infinite circular cylinders at arbitrary orientations,^{14,19,20} and polygon-based prisms with incident light rays parallel to the polygonal bases.²¹⁻²⁴ No ADT solution has been obtained for finite circular cylinders at arbitrary orientations. Moreover, much of the research related to ADT for nonspherical particles has not involved comparison with rigorous methods, except for spheres,¹³ spheroids,^{11,25} and infinite cylinders at random orientations,¹⁴ cubes,²³ and circular disks²⁴ with light incidence normal to the symmetry axis.

In the following sections, we present (1) a general approach for formulating ADT based on analytical geometry, (2) a formulation of ADT for finite cylinders, (3) an evaluation of our new ADT expressions for finite cylinders by comparison with rigorous *T*-matrix calculations, (4) further comparison of ADT solutions against rigorous *T*-matrix calculations for different cylinders so as to address whether some physical processes will lessen as particle shape becomes less spherical, and (5) implications for remote sensing and parameterization of cirrus clouds.

2. General Formulation of Anomalous Diffraction Theory

Van de Hulst coined the term anomalous diffraction to describe scattering phenomena based on two assumptions: (1) particle size parameter $x = 2\pi R/\lambda \gg 1$, where R is a characteristic dimension of the particle and λ is the wavelength of the electromagnetic wave in the surrounding medium; and (2) $|m - 1| \ll 1$, where $m = m_r - im_i$ is the complex refractive index of the particle relative to the medium whose refractive index is assumed to be unity. The first assumption implies geometrical optics; the second assumption implies that rays are negligibly deviated as they cross the particle boundary. Moreover, little energy is reflected at the boundary because the Fresnel reflection coefficients vanish when m approaches unity. In ADT, extinction is caused by absorption of light passing through the particle and by the interference of light passing through the particle and light passing around the particle. The integral form of ADT for arbitrarily shaped particles has been

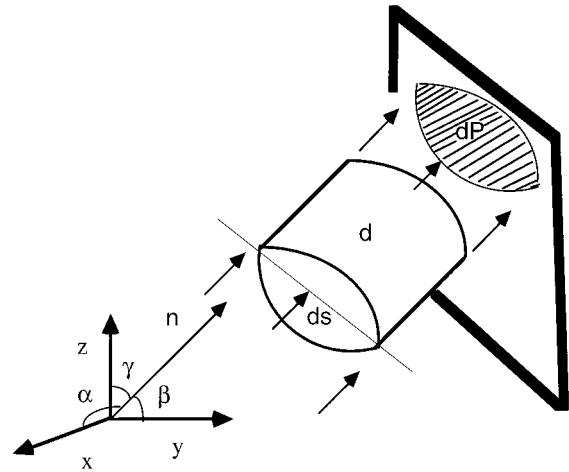


Fig. 1. Arbitrarily shaped particle and light rays characterized by the direction $\mathbf{n} = (\cos \alpha, \cos \beta, \cos \gamma)$.

described previously²⁰⁻²² and is the starting point for the general ADT analysis. As shown in Fig. 1, if d represents a ray path through the particle, then the phase shift suffered by this ray relative to a parallel ray traversing the same distance outside the particle is given by

$$\Phi = \frac{2\pi d}{\lambda} (m - 1). \quad (1)$$

The extinction cross section is given by

$$C_e = 2 \iint \text{Re}[1 - \exp(-i\Phi)] dP, \quad (2)$$

where Re represents the real part of a complex quantity, dP is the area element of the projection on the plane perpendicular to the direction of the light ray, and the integration is taken over the whole projected area P . The absorption cross section is given by

$$C_a = \iint \left[1 - \exp\left(-\frac{4\pi m_i d}{\lambda}\right) \right] dP \quad (3)$$

with the same integration domain.

Extinction and absorption cross sections can be obtained from Eqs. (1)–(3) by analytical derivations or at least by numerical integration if both the ray path d and the element of projected area dP can be expressed as functions of some integration variables such as x and y in the Cartesian coordinate system. When the cross sections are divided by the projected areas, the corresponding efficiencies can be obtained. In general, these functional relationships depend on particle shape and orientation. Given a specific particle shape and orientation, the challenge in formulating ADT is to find the ray path and the projected area. In finding the ray path and projected area, most previous studies used geometric arguments that are difficult to generalize for complicated particle geometries. Such difficulty may be the reason that analytical ADT results have been obtained only for

spheres, spheroids, and infinite circular cylinders at arbitrary orientations, as well as a few other shapes (such as cubes and prisms) at special orientations. Because ADT assumptions assure an undeviated propagation of light rays, analytical geometry can be used to find the ray path and the projected area.

We begin with the ray path. Consider a particle in the Cartesian coordinates as shown in Fig. 1. If the light propagation direction angles with respect to the x , y , and z axes are α , β , and γ , respectively, the corresponding unit vector of the direction is characterized by

$$\mathbf{n} = (n_x, n_y, n_z), \quad (4)$$

where $n_x = \cos \alpha$, $n_y = \cos \beta$, and $n_z = \cos \gamma$.

Suppose a ray enters the particle at the point (x_1, y_1, z_1) on the surface that is described by

$$f_1(x, y, z) = 0. \quad (5)$$

The line passing the point (x_1, y_1, z_1) with the direction (α, β, γ) satisfies the following set of linear equations:

$$x - x_1 = n_x t, \quad (6a)$$

$$y - y_1 = n_y t, \quad (6b)$$

$$z - z_1 = n_z t, \quad (6c)$$

where $t > 0$ is a distance parameter along the direction of the incident light.²⁶ If the ray exits the particle at the point (x_2, y_2, z_2) on the surface that can be described by

$$f_2(x, y, z) = 0, \quad (7)$$

then the ray path d is determined by the distance between the point (x_1, y_1, z_1) and the point (x_2, y_2, z_2) that is given by

$$d = [(x_2 - x_1)^2 + (y_2 - y_1)^2 + (z_2 - z_1)^2]^{1/2}. \quad (8a)$$

With (x_2, y_2, z_2) on the line determined by Eqs. (6), Eq. (8a) becomes

$$d = t(n_x^2 + n_y^2 + n_z^2)^{1/2} = t, \quad (8b)$$

where $(n_x^2 + n_y^2 + n_z^2)^{1/2} = 1$ is used. The quantity t can be found by solving Eqs. (6) and (7) as a function of (x_1, y_1, z_1) and (α, β, γ) . In other words, the ray path can be found for a given direction of incident light if the equations for surfaces where rays enter and exit are known.

The projected area, which uses only the surface equation where the ray enters, is easier to determine. The area element of the surface ds is readily obtained as it is solely determined by the surface equation described by Eq. (5). Also, the normal unit vector of this surface at an arbitrary point p_1 can be found through Eqs. (6) based on the following equation:

$$\mathbf{n}_s = \frac{(\nabla f_1)_{p_1}}{\|\nabla f_1\|_{p_1}}, \quad (9)$$

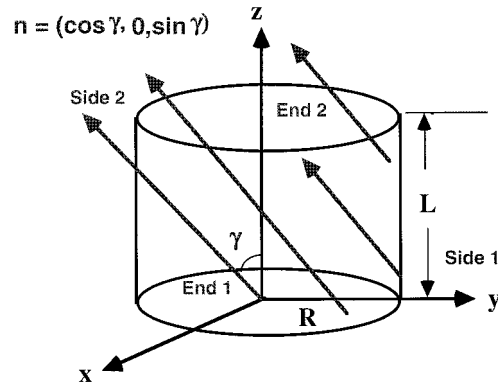


Fig. 2. Finite circular cylinder and light rays characterized by the direction $\mathbf{n} = (\sin \gamma, 0, \cos \gamma)$.

where ∇f represents the gradient of f and $\|\cdot\|$ represents the Euclidean norm.²⁷ The projected area element dP is then given by

$$dP = \mathbf{n} \cdot d\mathbf{s} = (\mathbf{n} \cdot \mathbf{n}_s)ds. \quad (10)$$

Therefore, for a given direction of incident light, the ADT solution can be obtained by use of surface equations where the ray enters and exits the particle. This method is used in the next section to derive the ADT for finite circular cylinders at arbitrary orientations.

3. New Anomalous Diffraction Theory Expressions for Finite Circular Cylinders

Spheroids are frequently studied nonspherical shapes. However, spheroids do not have sharp edges like those of some ice crystals. Unlike spheroids, finite cylinders are characterized by sharp, rectangular edges in partial analogy to hexagonal ice crystals. Previous results indicate that scattering properties of circular cylinders are different from those of spheroids in many aspects.^{28,29} The rigorous T -matrix code is available for calculating scattering properties of circular cylinders,^{5,28,29} and the exact T -matrix results can be used to evaluate approximate ADT results.

For finite cylinders, the difficulty in formulating ADT lies in the end effects (the end effects are ignored in formulating ADT for infinite cylinders and finite cylinders at normal incidence). As discussed above, the known surface equations can be used to formulate the ADT for a finite cylinder. As shown in Fig. 2, without loss of the generality, assume the rays enter End 1 and Side 1 and exit End 2 and Side 2. In terms of the ray path, the problem can be divided into four nonoverlapping parts: End 1 to Side 2, End 1 to End 2, Side 1 to Side 2, Side 1 to End 2. In the following subsections we discuss these in detail.

End 1 is described by

$$x^2 + y^2 = r^2, \quad (11a)$$

$$z = 0. \quad (11b)$$

The equation for End 2 is

$$x^2 + y^2 = r^2, \quad (12a)$$

$$z = L, \quad (12b)$$

where L is the length of the cylinder. The equation for the side is

$$x^2 + y^2 = R^2, \quad (13a)$$

$$0 \leq z \leq L, \quad (13b)$$

where R is the diameter of the cylinder.

A. End 1 to Side 2

Consider light rays that enter the cylinder from End 1 and exit from Side 2. The line that passes any point $p = (x, y, z)$ on End 1 with the direction $\mathbf{n} = (n_x, n_y, n_z)$ is described by Eqs. (6). Coupled with Eq. (13a) and inequality 13(b), the ray path is given by

$$d_1^{(1)} = \frac{-(n_x x + n_y y) \pm [(n_x^2 + n_y^2)(R^2 - r^2) + (n_y x + n_x y)^2]^{1/2}}{(n_x^2 + n_y^2)}, \quad (14a)$$

where the subscript 1 and superscript (1) together denote the contribution from End 1 to Side 2. Note that $|r(n_x \cos \phi + n_y \sin \phi)| \leq [r^2(n_x \cos \phi + n_y \sin \phi)^2 + (n_x^2 + n_y^2)(R^2 - r^2)]^{1/2}$ because $R \geq r$. Because the ray path is nonnegative, we choose only the solution given by

$$d_1^{(1)} = \frac{[(n_x^2 + n_y^2)(R^2 - r^2) + (n_y x + n_x y)^2]^{1/2} - (n_x x + n_y y)}{(n_x^2 + n_y^2)}. \quad (14b)$$

In the polar coordinates where $x = r \cos \phi$ and $y = r \sin \phi$,

$$d_1^{(1)} = \frac{[r^2(n_x \cos \phi + n_y \sin \phi)^2 + (n_x^2 + n_y^2)(R^2 - r^2)]^{1/2} - r(n_x \cos \phi + n_y \sin \phi)}{(n_x^2 + n_y^2)}. \quad (14c)$$

Equation (14c) can be simplified because of the symmetry of the circular cylinder. We can always choose rays that propagate in the direction parallel to the x - z plane, as has been applied in previous studies of an infinite cylinder^{14,19,20}, i.e.,

$$n_y = 0, \quad (15a)$$

$$n_x = \sin \gamma, \quad (15b)$$

$$n_z = \cos \gamma, \quad (15c)$$

where $0 \leq \gamma \leq \pi/2$.

The simplified expression for the ray path is

$$d_1^{(1)} = \frac{[R^2 - r^2 \sin^2 \phi]^{1/2} - r \cos \phi}{\sin \gamma}. \quad (16)$$

Because the normal direction of End 1 is $\mathbf{n}_s = (0, 0, 1)$, the projected area element is given by

$$dP = (\mathbf{n} \cdot \mathbf{n}_s) ds = r \cos \phi dr d\phi. \quad (17)$$

Therefore the extinction cross section for this part is given by

$$C_{e1}^{(1)} = 2 \cos \gamma \iint_{A_1} \{1 - \exp[-ik(m-1)d_1^{(1)}]\} \cdot r dr d\phi, \quad (18)$$

where A_1 is the integration domain that covers all the rays from End 1 to Side 2. As shown below, we do not need to explicitly know A_1 .

B. End 1 to End 2

Consider rays that enter the cylinder from End 1 and exit from the other end of the cylinder (End 2). This subproblem is analogous to consideration of a thin disk. The ray path is given by

$$d_1^{(2)} = \frac{L}{n_z} = \frac{L}{\cos \gamma}. \quad (19)$$

The surface area element is also given by Eq. (17). Therefore the extinction cross section for this part is given by

$$C_{e1}^{(2)} = 2 \cos \gamma \iint_{A_2} \{1 - \exp[-ik(m-1)d_1^{(2)}]\} r dr d\phi, \quad (20)$$

where A_2 is the integration domain that covers all the rays from End 1 to Side 2. As shown below, we do not need to explicitly know A_2 .

C. Side 1 to Side 2

Consider rays that enter the cylinder from Side 1 and exit from Side 2. This subproblem is similar to that of an infinite cylinder at arbitrary orientations. The ray path is given by

$$d_2^{(1)} = \frac{-2(n_x x + n_y y)}{(n_x^2 + n_y^2)}, \quad (21a)$$

and in polar coordinates is

$$d_2^{(1)} = \frac{-2R(n_x \cos \phi + n_y \sin \phi)}{(n_x^2 + n_y^2)}. \quad (21b)$$

By use of the symmetry condition given by Eqs. (15), Eq. (21b) is reduced to

$$\mathbf{d}_2^{(1)} = \frac{2R \cos \phi}{\sin \gamma}. \quad (21c)$$

Note that the minus sign was eliminated for clarity by choosing the coordinate system such that the incident rays are in the domain determined by

$$-\frac{\pi}{2} \leq \phi \leq \frac{\pi}{2}. \quad (21d)$$

The normal direction of Side 1 is given by

$$\mathbf{n}_s = \left(\frac{x_1}{R}, \frac{y_1}{R}, 0 \right). \quad (22)$$

Therefore the projected area element is given by

$$dP = -(\mathbf{n} \cdot \mathbf{n}_s) ds = R \sin \gamma \cos \phi d\phi dz. \quad (23)$$

The extinction cross section for this part is given by

$$C_{e2}^{(1)} = 2R \sin \gamma \iint_{A_3} \{1 - \exp[-ik(m-1)d_2^{(1)}]\} \\ \times \cos \phi dz d\phi, \quad (24)$$

where A_3 is the integration domain that covers all the rays from Side 1 to Side 2. As shown below, we do not need to know A_3 explicitly.

D. Side 1 to End 2

Consider that rays enter the cylinder from Side 1 and exit from End 2. In this case, the ray path can be found by solving a line equation passing a point (x, y, z) on Side 1 described by Eq. (13a) and inequality 13(b) coupled with Eqs. (6):

$$d_2^{(2)} = \frac{L-z}{\cos \gamma}. \quad (25)$$

Combined with Eq. (23) for the projected area element, the extinction cross section can be given by

$$C_{e2}^{(2)} = 2R \sin \gamma \iint_{A_4} \{1 - \exp[-ik(m-1)d_2^{(2)}]\} \\ \times \cos \phi dz d\phi, \quad (26)$$

where A_4 is the integration domain that covers all the rays from Side 1 to End 2. As shown below, we do not need to explicitly know A_4 .

E. Addition Theorem: Total Extinction and Absorption

With contributions from each part, total extinction and absorption can be determined by use of the so-called addition theorem.^{21,22} Briefly, a particle can be divided into a number of segments with the non-overlapping projected area using planes parallel to the incident light rays. As a result of the additivity of the integration, the extinction, absorption, and scattering cross sections of the whole particle can be

expressed as a sum of the contributions from each individual segment. Based on the addition theorem, the contributions from the rays incident to End 1 are given by

$$C_{e1} = \sum_{j=1}^2 C_{e1}^{(j)} \\ = 2 \cos \gamma \int_0^{2\pi} d\phi \int_0^R dr \{1 - \exp[-ik(m-1)d_1]\} r, \quad (27a)$$

where

$$d_1 = \begin{cases} d_1^{(1)}, & \text{if } d_1^{(1)} \cos \gamma \leq L \\ d_1^{(2)}, & \text{if } d_1^{(1)} \cos \gamma > L \end{cases}. \quad (27b)$$

Note that the integration domain is given by $A_1 + A_2 = (0 \leq r \leq R; 0 \leq \phi \leq 2\pi)$.

Similarly, the contribution from Side 1 is given by

$$C_{e2} = \sum_{j=1}^2 C_{e2}^{(j)} \\ = 2R \sin \gamma \int_0^L dz \int_{-\pi/2}^{\pi/2} d\phi \\ \times \{1 - \exp[-ik(m-1)d_2]\} \cos \phi, \quad (28a)$$

$$d_2 = \begin{cases} d_2^{(1)}, & \text{if } z + d_2^{(1)} \cos \gamma \leq L \\ d_2^{(2)}, & \text{if } z + d_2^{(1)} \cos \gamma > L \end{cases}. \quad (28b)$$

Note that the integration domain is given by $A_3 + A_4 = (0 \leq z \leq L; -\pi/2 \leq \phi \leq \pi/2)$. The total extinction cross section of the cylinder is given by

$$C_e = \sum_{j=1}^2 C_{ej}. \quad (29)$$

The absorption cross section can be obtained by substituting the corresponding ray path and projected area element into Eq. (3).

We have described how to obtain the extinction and absorption cross sections of an arbitrary cylinder at arbitrary orientations. Corresponding efficiencies can easily be found by dividing each cross section with the corresponding projected area. Next we discuss efficiencies averaged over random orientations.

F. Random Orientation Average

With the ADT solution for an arbitrary cylinder at arbitrary orientations, the cross section can be expressed as

$$\bar{C} = \int_0^{\pi/2} C(\gamma) \sin \gamma d\gamma, \quad (30)$$

where \bar{C} can be either the extinction or the absorption cross section.⁶ For a circular cylinder with the cyl-

inder radius R and length L , the randomly averaged projected area is

$$P = \frac{\pi}{2}RL + \frac{\pi}{2}R^2 = \pi R^2 \left(\frac{2 + \varepsilon}{2\varepsilon} \right), \quad (31a)$$

where the diameter-to-length ratio is defined as

$$\varepsilon = (2R/L). \quad (31b)$$

Efficiencies are given by

$$Q = (\bar{C}/P). \quad (32)$$

We have shown how to obtain the integral ADT expressions for a finite circular cylinder at arbitrary and random orientations. The ADT efficiencies can be computed by numerical integration of the corresponding equations.

4. Evaluation of Anomalous Diffraction Theory

We have shown the ADT expressions for an arbitrary cylinder. Our new expressions are justified by studying special cases that have known solutions.

A. Cases in which End Effects can be Ignored

The ADT solutions for finite cylinders normal to the incident light¹³ and for infinite cylinders at oblique incidence^{14,19,20} are available. Our new ADT for finite cylinders reduces to both special cases when corresponding conditions are satisfied.

For a finite cylinder at the normal incidence, when the light rays enter and exit the sides of the cylinder, $\gamma = \pi/2$ leads to

$$n_z = \cos \gamma = 0. \quad (33)$$

Substitution of Eq. (33) into Eq. (20) indicates that the contribution from End 1 is zero. Also, we have

$$d_2 = d_2^{(1)} \quad (34)$$

because $z \leq L$ holds no matter what value z is in the range of $0 \leq z \leq L$. Therefore, for normal incidence,

$$C_e = 4RL \operatorname{Re} \int_0^{\pi/2} \{1 - \exp[-i2Rk(m-1) \times \cos \phi]\} \cos \phi d\phi. \quad (35)$$

Dividing by the projected area $P = 2RL$, the extinction efficiency can be given by

$$Q_e = 2 \operatorname{Re} \int_0^{\pi/2} [1 - \exp(-i\rho^* \cos \phi)] \cos \phi d\phi, \quad (36a)$$

$$\rho^* = 2kR(m-1). \quad (36b)$$

Equations (36a) and (36b) are identical with van de Hulst's result.¹³

For an infinite cylinder, the end effects are ignored.

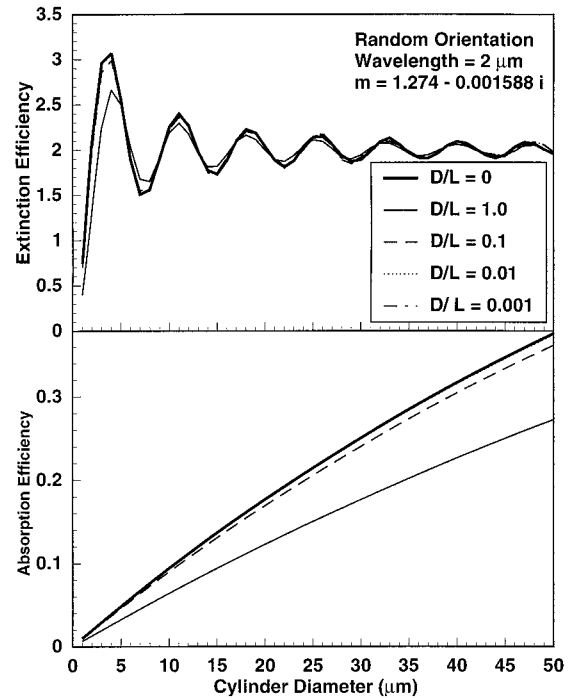


Fig. 3. ADT extinction and absorption efficiencies for randomly oriented cylinders having a variety of aspect ratios. Note that efficiencies approach those of infinite cylinders as the D/L ratio decreases. The curves for the 0.01 and 0.001 D/L ratios are almost the same as the infinite cylinder results. All the curves were computed by use of the new ADT.

Only a Side 1 to Side 2 contribution exists. Therefore

$$C_e = 4RL \sin \gamma \operatorname{Re} \left\{ \int_0^{\pi/2} \left[1 - \exp \left(-i\rho^* \frac{\cos \phi}{\sin \gamma} \right) \right] \times \cos \phi d\phi \right\}. \quad (37)$$

Dividing by the projected area $P(\gamma) = 2RL \sin \gamma$, the extinction efficiency at the oblique angle γ can be given by

$$Q_e(\gamma) = 2 \operatorname{Re} \left\{ \int_0^{\pi/2} \left[1 - \exp \left(-i\rho^* \frac{\cos \phi}{\sin \gamma} \right) \right] \cos \phi d\phi \right\}. \quad (38)$$

This result is consistent with previous research.¹⁷

Our new ADT expressions can also be used to evaluate the gradual change from a finite cylinder to an infinite cylinder. This is demonstrated in Fig. 3 in terms of randomly averaged extinction and absorption efficiencies. Figure 3 shows that both absorption and extinction efficiency are mostly sensitive to a diameter-to-length (D/L) ratio larger than 0.1. The infinite cylinder provides reasonable approximation to a finite cylinder with a D/L ratio less than 0.01. This result is similar to the result obtained in Refs. 27 and 28.

B. Comparison of the Anomalous Diffraction Theory with T -Matrix Calculations

Although ADT has been widely used, systematic comparison with rigorous results has been limited to spheres,¹³ infinite cylinders,¹⁹ and spheroids.^{11,25} To evaluate our ADT expressions for finite cylinders, we further compare ADT calculations with the T -matrix calculations.

The mathematical details of the T -matrix approach have been previously discussed.^{5,6} The T -matrix method solves light-scattering problems by expanding the fields (incident, internal, and scattering) in terms of eigenfunctions, i.e., basis functions that are solutions of the electromagnetic wave equations. The coefficients of the incident field expansion functions are determined by the given incident field. The coefficients of the scattered and internal field expansion functions can be determined by applying the electromagnetic boundary conditions to the governing Maxwell's equations. If \mathbf{a} is the coefficient vector of the incident field, \mathbf{b} is the coefficient vector of the internal field, and \mathbf{c} is the coefficient vector of the scattering field, then these coefficient vectors are related by

$$\mathbf{b} = \mathbf{Q}_1^{-1}\mathbf{a}, \quad (39a)$$

$$\mathbf{c} = \mathbf{Q}_2\mathbf{b}, \quad (39b)$$

$$\mathbf{c} = \mathbf{T}\mathbf{a}, \quad (39c)$$

$$\mathbf{T} = \mathbf{Q}_2\mathbf{Q}_1^{-1}, \quad (39d)$$

where the matrices \mathbf{Q}_1 and \mathbf{Q}_2 are determined by the surface integrals, \mathbf{Q}_1^{-1} is the inverse of \mathbf{Q}_1 , and \mathbf{T} is the transition matrix. A fundamental feature of the T -matrix approach is that the elements of the T -matrix are independent of the incident and scattered fields and depend only on the shape, size parameter, and refractive index of the scattering particle as well as its orientation with respect to the coordinate system. Consequently, the transition matrix needs to be computed only once and then can be used for any direction of light incidence and scattering. In principle, the T -matrix method can be applied to any particle shape. However, virtually all available codes assume axisymmetric particles (e.g., spheroids, Chebyshev particles, and circular cylinders). We compare the T -matrix calculation with the ADT for finite cylinders.

The ADT assumptions assure that its solution is close to the corresponding T -matrix calculation when the refractive index approaches 1. To demonstrate this, we chose a wavelength of $2.865 \mu\text{m}$ with a refractive index of $1.0036 - 0.0923i$ (ice). Figure 4 shows the results of extinction efficiency and absorption efficiency for randomly oriented cylinders with a D/L ratio of 1.0. Figure 5 shows the results for randomly oriented cylinders with a D/L ratio of 2.5.

Previous studies have shown that ADT produces a correct phase in the extinction efficiency curve as a function of size parameter for spheres,¹³ randomly oriented infinite cylinders,¹⁴ and randomly oriented

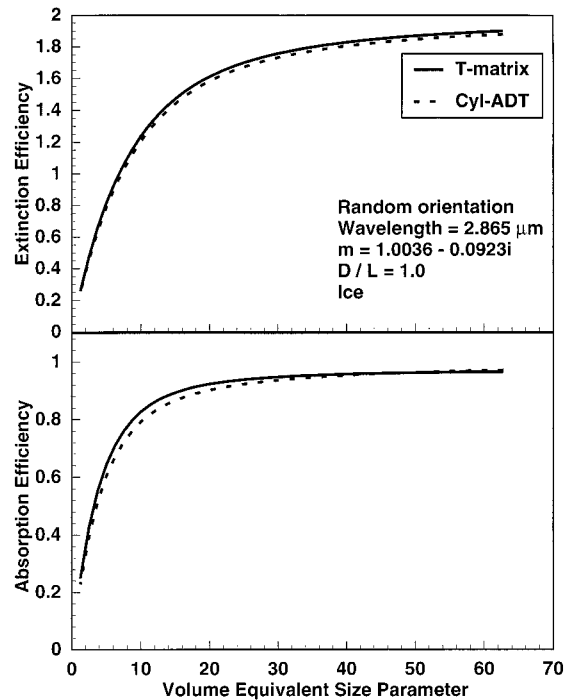


Fig. 4. ADT efficiencies for a randomly oriented cylinder. Note that cylinder ADT approaches T -matrix calculations when the real part of the refractive index is close to 1.0. The D/L ratio is 1.0.

spheroids.²⁵ Figure 6 demonstrates that our new ADT for randomly oriented cylinders produces the same phase agreement for extinction. A wavelength of $2 \mu\text{m}$ was selected to show an example in which ADT diverges from the exact T -matrix result because of the relatively large real refractive index (1.274)

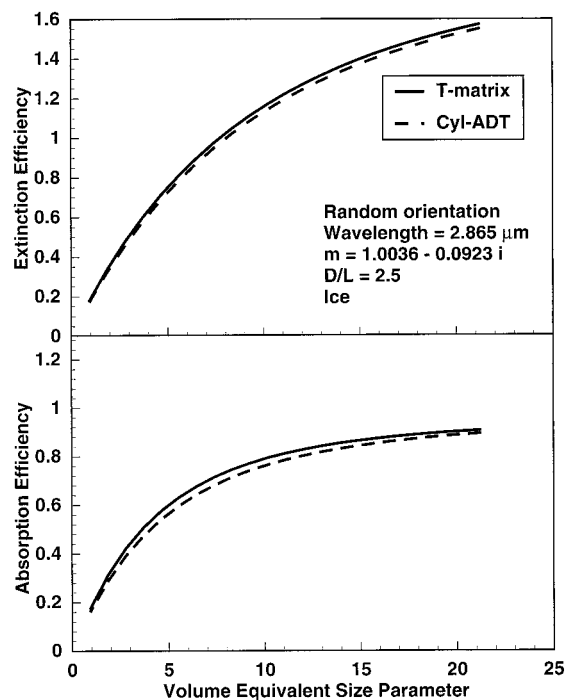


Fig. 5. Same as Fig. 4, except that the D/L ratio is 2.5.

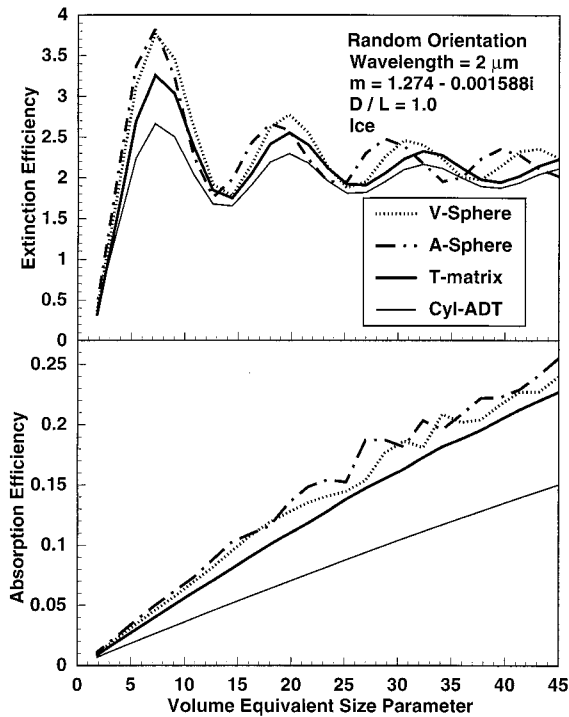


Fig. 6. Efficiencies calculated from cylinder ADT (solid curve), volume-equivalent spheres (dotted curve), area-equivalent spheres (dashed-dotted curve), and the T -matrix method (heavy solid curve). The D/L ratio is 1.0, the wavelength is $2 \mu\text{m}$, and the refractive index is $1.274 - 0.001588i$. Mie theory was used for the spheres.

and relatively small imaginary refractive index (0.001588). Note in Fig. 6(b) that Mie theory slightly overestimates the absorption efficiency, whereas ADT provides a substantial underestimate.

5. Nonsphericity Influence on the Accuracy of Anomalous Diffraction Theory

ADT considers the transmitted light but ignores scattering processes such as internal reflection and refraction, edge effects, and tunneling effects. For spheres, Ackerman and Stephens¹⁵ improved the performance of van de Hulst's original ADT by empirically taking into account the contributions of internal reflection and refraction as well as edge effects. Their results indicated that the modified ADT mainly improved ADT performance for large size parameters. Similar efforts were made to modify the original ADT extinction for spheroids.^{16,17} Empirical functions are also given in Refs. 16 and 17 that bridge the Rayleigh and ADT extinction to improve the ADT performance in the small particle range. However, performance in the so-called resonance region with particle size comparable to wavelength, where errors of both the ADT and the equivalent sphere approach tend to be large,³⁰ is not easy to improve empirically.

In addition to the value in evaluating and modifying the ADT, comparisons of ADT with exact solutions for particles of different shapes are also useful for determining whether some physical processes will

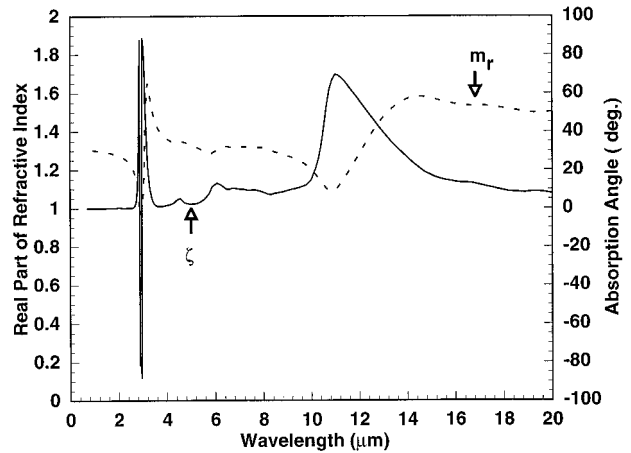


Fig. 7. Real refractive index and absorption angle for ice as a function of wavelength.

dampen or disappear with nonsphericity. Chylek *et al.*³⁰ assumed that surface waves responsible for resonances present in scattering by spherical particles are absent in scattering by irregular particles at random orientations. They proposed a method to eliminate the resonance effects that are due to these surface waves in the Mie series and obtained results in agreement with experimental data on phase functions. Recently, Baran *et al.*¹¹ compared ADT solutions with T -matrix calculations for both oblate and prolate spheroids. They argued that ADT provides better approximations than equivalent spheres for ice particles and addressed the question of nonspherical scattering by comparing ADT with rigorous solutions and the implications for remote sensing of cirrus clouds. However, their study was only for spheroids, and it appears that Baran *et al.* used an approximate ADT version given in Ref. 1 rather than the formal ADT solution for spheroids. To extend such studies, we compare the results obtained with our new ADT (derived from the original van de Hulst's assumptions) with the rigorous T -matrix calculations for finite cylinders having different D/L ratios.

It is well known that ADT performance depends on both real and imaginary refractive index. Van de Hulst¹³ introduced an absorption angle to characterize absorption strength:

$$\zeta = \tan^{-1} \left(\frac{m_i}{m_r - 1} \right). \quad (40)$$

Unlike the imaginary refractive index that characterizes absolute absorption, the absorption angle characterizes the absorption strength relative to the real refractive index. Following Ackerman and Stephens¹⁵, we use this unique quantity to characterize absorption strength. Figure 7 shows the absorption angle and real part of the refractive index for ice as a function of wavelength.³¹ Ackerman and Stephens¹⁵ classified absorption into no absorption ($\zeta = 0^\circ$), weak absorption ($\zeta = 0.2^\circ$), and strong absorption ($\zeta \geq 30^\circ$).

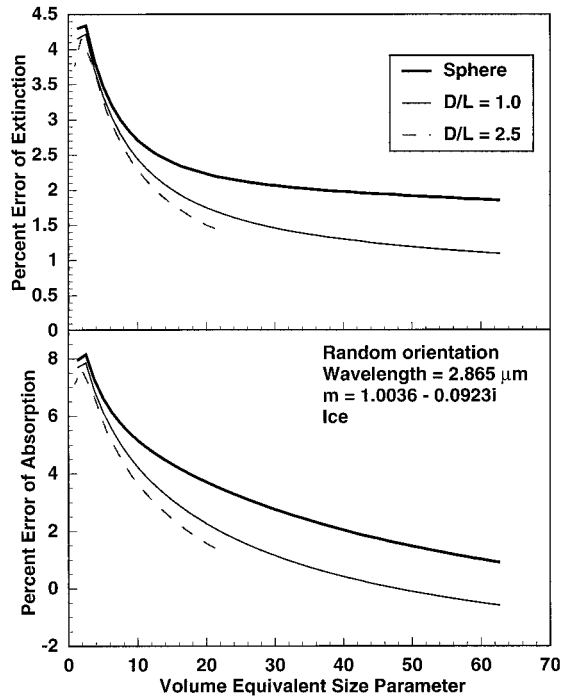


Fig. 8. Error of ADT approximations. Mie theory and van de Hulst's ADT for spheres were applied to spheres. The T -matrix method and the new ADT were used for cylinders.

To address the effects of the refractive index, we report results at three typical wavelengths. The 2.865- μm wavelength with $\zeta = 87.8$ and $m_r = 1.0036$ corresponds to strong absorption but small real refractive index; the 12.5- μm wavelength with $\zeta = 47.6$ and $m_r = 1.3857$ corresponds to strong absorption and large real refractive index; and the 2.2201- μm wavelength with $\zeta = 0.0486$ and $m_r = 1.2604$ corresponds to weak absorption. We present the results in terms of percent error between the ADT and the corresponding exact solution defined as

$$\delta = 100 \frac{Q_{\text{exact}} - Q_{\text{ADT}}}{Q_{\text{exact}}}, \quad (41)$$

where Q_{exact} represents Mie solutions for spheres and T -matrix solutions for finite cylinders, and Q_{ADT} represents solutions obtained by van de Hulst's ADT for spheres and those obtained by our new ADT for finite cylinders. We do not take the absolute value of the percent error, because the sign (positive or negative) provides additional information about whether ADT overestimates (negative) or underestimates (positive) exact values.

Figure 8 shows the ADT error as a function of volume-equivalent size parameter at the 2.865- μm wavelength for spheres as well as randomly oriented compact ($D/L = 1.0$) and platelike cylinders ($D/L = 2.5$). This figure shows that the differences between the ADT and the corresponding exact solutions decline with deviation from sphericity for both extinction and absorption in a broad size parameter range (from approximately 1 to 60). Furthermore,

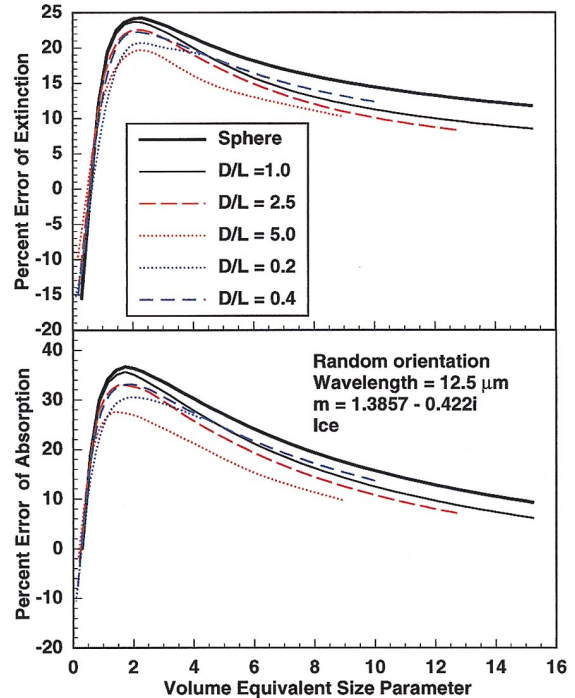


Fig. 9. Same as Fig. 8, except that the wavelength is 12.5 μm .

Fig. 8 indicates that similar to previous studies for spheres, infinite cylinders, and spheroids, our cylinder ADT approximates extinction better than absorption. Figure 8 also suggests that ADT is particularly suitable for approximating nonspherical scattering in the Christiansen bands with large absorption angle.

Figure 9 shows the ADT error at the 12.5- μm wavelength for spheres and a wide range of randomly oriented cylinders as a function of volume-equivalent size parameter. Columnlike cylinders have a D/L ratio < 1.0 . Figure 9 suggests that the ADT for columnlike cylinders is less accurate than that for platelike cylinders; similar findings for spheroids were reported recently in Ref. 11.

So far we have discussed results at wavelengths of relatively strong absorption. Figure 10 presents the results for a weak absorption case at the 2.2201- μm wavelength. Compared with strong absorption cases in which the resonance-induced ripple structure diminishes even for equivalent spheres, two points are of note. First, nonsphericity and orientation averaging reduce the ripple structure in both extinction and absorption. Second, ADT extinction errors diminish in relation to nonsphericity with increasing size parameter, whereas ADT absorption errors for cylinders tend to be in the middle of ADT errors for spheres that fluctuate with ripple structure.

It is well known that real refractive index plays an important role in morphology-dependent resonances.^{32,33} To see the effect of real refractive index, we combine the results at 2.865- and 12.5- μm wavelengths in Fig. 11. We define a new quantity Δ that

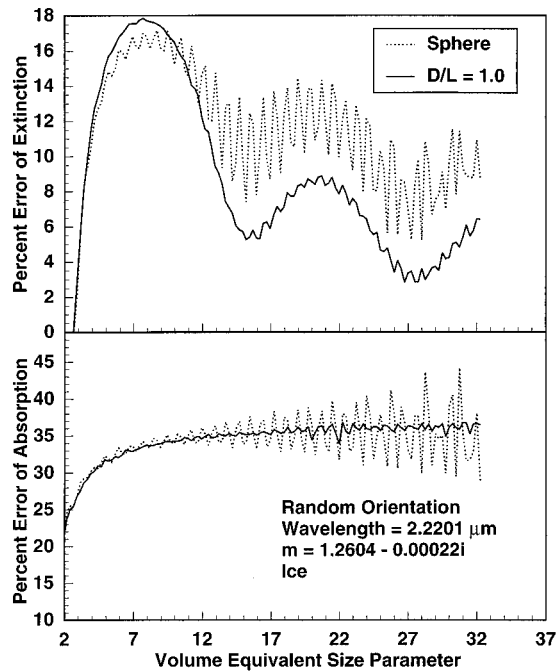


Fig. 10. Same as Fig. 8, except that the wavelength is 2.2201 μm . Note that results of a size parameter less than 2, where ADT tends to overestimate the efficiencies, are not shown to emphasize the ripple structure.

characterizes the relative change of δ from volume-equivalent spheres to cylinders:

$$\Delta = 100 \frac{\delta_{\text{Mie}} - \delta_{\text{ADT}}}{\delta_{\text{Mie}}} \quad (42)$$

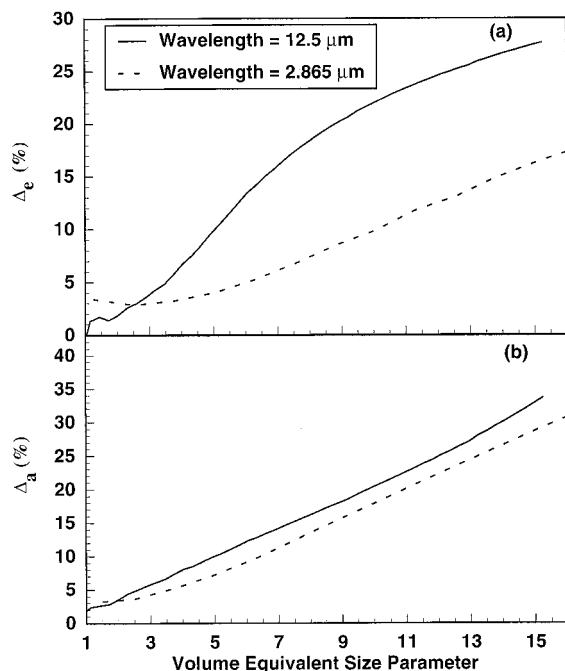


Fig. 11. Relative change of ADT error reduction when particle shapes change from spheres to compact cylinders with an aspect ratio of 1: (a) extinction, (b) absorption. See the text for the meaning of Δ_e and Δ_a .

A positive Δ implies error reduction of ADT with nonsphericity, and $\Delta = 100$ implies no ADT error for the nonspherical particles. In this case, δ_{Mie} is the percent error between a Mie and an ADT sphere, and δ_{ADT} is the percent error between the T -matrix and the ADT for finite cylinders. Figure 11 suggests that ADT error reduction with nonsphericity reduction at $\lambda = 12.5 \mu\text{m}$ is larger than that at $\lambda = 2.865 \mu\text{m}$ for both extinction and absorption. This is likely due to the larger real refractive index at $\lambda = 12.5 \mu\text{m}$ that generates stronger resonance effects.³³

As shown in Fig. 7, ice exhibits relatively strong absorption at wavelengths in the atmospheric window region (8–15 μm). This window region is important because it corresponds to strong terrestrial radiation partially escaping to space, and it has been used in remote sensing of aerosol and cloud properties.³⁴ Considering that both aerosol and ice particles are generally nonspherical, the value of using ADT in cloud parameterization and remote sensing is evident. In evaluating scattering by nonspherical particles, it is still common to apply Mie theory to equivalent spheres.³⁵ Our results suggest that ADT might serve as a better approximation than equivalent spheres in problems concerning scattering by nonspherical particles in the Christiansen bands and/or where absorption is relatively strong. ADT is expected to be a better approximation because the ripple that exists for a sphere will be averaged out for randomly oriented nonspherical particles.

6. Concluding Remarks

Based on analytical geometry, we developed a general ADT method for formulating extinction and absorption by nonspherical particles at arbitrary orientations. This method uses surface equations where the light rays enter and exit the particle and simplifies the ADT formulation for nonspherical particles. The ADT for finite circular cylinders was formulated by use of this new method. It has been analytically shown that our expressions reduce to those for an infinite cylinder when the cylinder is sufficiently long. The ADT for cylinders was further evaluated by our comparing results with the T -matrix calculations when the refractive index is close to 1. The ADT extinction curve is in phase with the T -matrix calculations even when the real refractive index is large and the ADT assumptions are violated.

By comparing ADT results with T -matrix calculations at different D/L ratios, we evaluated whether the error of the ADT approximation decreases with nonsphericity. Comparisons were made for three typical wavelengths representing (1) relatively strong absorption but small real refractive index, (2) relatively strong absorption and large real refractive index, and (3) weak absorption. First, we found that when absorption is strong, the error of ADT extinction and absorption decreases somewhat with deviation from sphericity over a broad size range. This suggests that some physical processes that exist for spherical scattering may dampen slightly with non-

sphericity. Second, when absorption is weak, ADT extinction error decreases with nonsphericity, whereas ADT absorption error does not. These results suggest that, in addition to the real refractive index, the absorption angle that essentially characterizes the ratio of imaginary to real refractive index plays an important role in addressing the issue of such so-called missing physics. Third, ADT in general approximates extinction better than absorption. Together with the second point, this suggests differing effects of nonsphericity on absorption and scattering processes.

In approximating extinction and absorption efficiency of nonspherical particles, equivalent sphere and ADT approaches exhibit significant differences. First, ADT approaches exact solutions as the refractive index approaches unity, which makes ADT a good tool for use in the Christiansen bands.³⁶ Equivalent sphere approximations for nonspherical particles do not have such features. Second, ADT variation with size parameter is in phase with that of exact solutions, whereas equivalent spheres are usually out of phase. Third, for wavelengths of strong absorption, ADT error in both extinction and absorption decreases slightly with nonsphericity, in contrast to the equivalent sphere approximation in which error increases with nonsphericity. These contrasts between the ADT and the equivalent sphere approach may lead to differences in the results of remote sensing of cirrus clouds. In Ref. 11, for example, Baran *et al.* found that the size of ice crystals obtained using ADT was much larger than that obtained using the equivalent sphere approximation. Although we found that the ADT approximation is somewhat better for nonspherical ice particles (particularly for the Christiansen bands), ADT should be used with caution. Our methodology is useful as a tool for determining the error in using ADT for nonspherical particles and has the potential of extending to other particle geometries.

This research was supported by the National Science Foundation grant ATM-9413437. We acknowledge helpful discussions with D. L. Mitchell and P. W. Barber at the Desert Research Institute. We gratefully acknowledge M. I. Mishchenko at the Goddard Space Flight Center of the National Aeronautics and Space Administration for providing the *T*-matrix code. Some calculations presented in this paper were made on a supercomputer at the National Center for Atmospheric Research.

References

1. D. L. Mitchell and W. P. Arnott, "A model predicting the evolution of ice particle size spectra and radiative properties of cirrus clouds. Part II: Dependence of absorption and extinction on ice crystal morphology," *J. Atmos. Sci.* **51**, 817–832 (1994).
2. D. L. Mitchell, A. Macke, and Y. Liu, "Modeling cirrus clouds. Part II: Treatment of radiative properties," *J. Atmos. Sci.* **53**, 2967–2988 (1996).
3. Q. Fu and K. N. Liou, "Parameterization of the radiative properties of cirrus clouds," *J. Atmos. Sci.* **50**, 2008–2025 (1993).
4. W. P. Arnott, C. Schmitt, Y. Liu, and J. Hallett, "Droplet size spectra and water-vapor concentration of laboratory water clouds: inversion of Fourier transform infrared (500–5000 cm^{-1}) optical-depth measurement," *Appl. Opt.* **36**, 5205–5216 (1997).
5. M. I. Mishchenko, L. D. Travis, and D. W. Mackowski, "T-matrix computations of light scattering by nonspherical particles: a review," *J. Quant. Spectrosc. Radiat. Transfer* **55**, 535–575 (1996).
6. P. W. Barber and S. C. Hill, *Light Scattering by Particles: Computational Methods* (World Scientific, Singapore, 1990).
7. P. W. Barber and H. Massoudi, "Recent advances in light scattering calculations for nonspherical particles," *Aerosol Sci. Technol.* **1**, 303–315 (1982).
8. M. I. Mishchenko, L. D. Travis, R. A. Kahn, and R. A. West, "Modeling phase functions for dustlike tropospheric aerosols using shape mixture of randomly oriented polydisperse spheroids," *J. Geophys. Res.* **D102**, 16831–16847 (1997).
9. S. Kinne and K. N. Liou, "The effects of the nonsphericity and size distribution of ice crystals on the radiative properties of cirrus clouds," *Atmos. Res.* **24**, 273–284 (1989).
10. P. Yang, K. N. Liou, and W. P. Arnott, "Extinction efficiency and single-scattering albedo for laboratory and natural cirrus clouds," *J. Geophys. Res.* **D102**, 21825–21835 (1997).
11. A. J. Baran, J. S. Foot, and D. L. Mitchell, "Ice crystal absorption: a comparison between theory and implications for remote sensing," *Appl. Opt.* **37**, 2207–2215 (1998).
12. W. P. Arnott, Y. Liu, and J. Hallett, "Unreasonable effectiveness of mimicking measured infrared extinction by hexagonal ice crystals with Mie ice spheres," in *Optical Remote Sensing of the Atmosphere*, Vol. 5 of 1997 Technical Digest Series (Optical Society of America, Washington, D.C., 1997), 216–218.
13. H. C. van de Hulst, *Light Scattering by Small Particles* (Wiley, New York, 1957).
14. G. L. Stephens, "Scattering of plane waves by soft obstacles: anomalous diffraction theory for circular cylinders," *Appl. Opt.* **23**, 954–959 (1984).
15. S. A. Ackerman and G. L. Stephens, "The absorption of solar radiation by cloud droplets: an application of anomalous diffraction theory," *J. Atmos. Sci.* **44**, 1574–1588 (1987).
16. G. R. Fournier and B. T. N. Evans, "Approximation to extinction efficiency for randomly oriented spheroids," *Appl. Opt.* **30**, 2042–2048 (1991).
17. B. T. N. Evans and G. R. Fournier, "Analytic approximation to randomly oriented spheroid extinction," *Appl. Opt.* **33**, 5796–5805 (1994).
18. J. M. Breenberg and A. S. Meltzer, "The effects of orientation of non-spherical particles on interstellar extinction," *Astrophys. J.* **132**, 667–671 (1960).
19. F. D. Bryant and P. Latimer, "Optical efficiencies of large particles of arbitrary shape and orientation," *J. Colloid Interface Sci.* **30**, 291–304 (1969).
20. D. A. Cross and P. Latimer, "General solutions for the extinction and absorption efficiencies of arbitrarily oriented cylinders by anomalous-diffraction methods," *J. Opt. Soc. Am.* **60**, 904–907 (1970).
21. P. Chylek and J. D. Klett, "Extinction cross sections of nonspherical particles in the anomalous diffraction approximation," *J. Opt. Soc. Am. A* **8**, 274–281 (1991).
22. P. Chylek and J. D. Klett, "Absorption and scattering of electromagnetic radiation by prismatic columns: anomalous diffraction approximation," *J. Opt. Soc. Am. A* **8**, 1713–1720 (1991).
23. A. Maslowska, P. J. Flatau, and G. L. Stephens, "Scattering of light by cubes: anomalous diffraction and discrete dipole approximations," *IRS' 92 Current Problems in Atmospheric Radi-*

- ation, S. Keevallik and O. Kärner, eds. (Deepak, Hampton, Va., 1992), 533–535.
24. P. Chylek and G. Videen, “Longwave radiative properties of polydispersed hexagonal ice crystals,” *J. Atmos. Sci.* **51**, 175–190 (1994).
 25. S. Asano and M. Sato, “Light scattering by randomly oriented spherical particles,” *Appl. Opt.* **19**, 962–974 (1980).
 26. A. Bowyer and J. Woodwark, *A Programmer’s Geometry* (Butterworth, London, 1983).
 27. R. L. Burden and J. D. Faires, *Numerical Analysis* (PWS-Kent, Boston, Mass., 1993).
 28. M. I. Mishchenko, L. D. Travis, and A. Macke, “Scattering of light by polydisperse, randomly oriented, finite circular cylinders,” *Appl. Opt.* **35**, 4927–4940 (1996).
 29. R. D. Haracz, L. D. Cohen, and A. Cohen, “Scattering of linearly polarized light from randomly oriented cylinders and spheroids,” *J. Appl. Phys.* **58**, 3322–3327 (1985).
 30. P. C. Chylek, G. W. Grams, and R. G. Pinnick, “Light scattering by irregular randomly oriented particles,” *Science* **193**, 480–482 (1976).
 31. S. Warren, “Optical constants of ice from the ultraviolet to the microwave,” *Appl. Opt.* **23**, 1206–1225 (1984).
 32. S. C. Hill and B. E. Benner, “Morphology-dependent resonances,” in *Optical Effects Associated with Small Particles*, P. W. Barber and P. K. Change, eds. (World Scientific, Singapore, 1988).
 33. L. G. Guimaraes and H. M. Nussenzveig, “Theory of Mie resonances and ripple fluctuations,” *Opt. Commun.* **89**, 363–369 (1992).
 34. S. A. Ackerman, “Remote sensing aerosols using satellite infrared observations,” *J. Geophys. Res. D* **102**, 17069–17079 (1997).
 35. H. M. Steele and R. P. Turco, “Retrieval of aerosol size distributions from satellite extinction spectra using constrained linear inversion,” *J. Geophys. Res. D* **102**, 16737–16747 (1997).
 36. W. P. Arnott, Y. Dong, and J. Hallett, “Extinction efficiency in the infrared (2–18 μm) of laboratory ice clouds: observations of scattering minima in the Christiansen bands of ice,” *Appl. Opt.* **34**, 541–551 (1995).